Journal of Luminescence 177 (2016) 266–274

Contents lists available at ScienceDirect

Journal of Luminescence

journal homepage: www.elsevier.com/locate/jlumin

Full Length Article

Nanoscale nonlinear effects in Erbium-implanted Yttrium Orthosilicate

Nadezhda Kukharchyk [a,b,*], Stepan Shvarkov [c], Sebastian Probst [d], Kangwei Xia [e], Hans-Werner Becker [f], Shovon Pal [b,g], Sergej Markmann [g], Roman Kolesov [e], Petr Siyushev [e], Jörg Wrachtrup [e], Arne Ludwig [b], Alexey V. Ustinov [h], Andreas D. Wieck [b], Pavel Bushev [a,**]

[a] *Experimentalphysik, Universität des Saarlandes, D-66123 Saarbrücken, Germany*
[b] *Angewandte Festkörperphysik, Ruhr-Universität Bochum, D-44780 Bochum, Germany*
[c] *Optoelektronische Materialien und Bauelemente, Universität Paderborn, D-33098 Padeborn, Germany*
[d] *Quantronics group, Service de Physique de l'Etat Condense, DSM/IRAMIS/SPEC, CNRS UMR 3680, CEA-Saclay, 91191 Gif-sur-Yvette cedex, France*
[e] *3. Physikalisches Institut, Universität Stuttgart, D-70569 Stuttgart, Germany*
[f] *RUBION, Ruhr-Universität Bochum, D-44780 Bochum, Germany*
[g] *AG THz Spectroscopie und Technologie, Ruhr-Universität Bochum, D-44780 Bochum, Germany*
[h] *Physikalisches Institut, Karlsruhe Institute of Technology, D-76128 Karlsruhe, Germany*

ARTICLE INFO

Article history:
Received 21 September 2015
Received in revised form
19 April 2016
Accepted 3 May 2016
Available online 7 May 2016

Keywords:
Rare earth
Ion implantation
Resonance energy exchange
Erbium
Concentration dependence

ABSTRACT

Doping of substrates at desired locations is a key technology for spin-based quantum memory devices. Focused ion beam implantation is well-suited for this task due to its high spacial resolution. In this work, we investigate ion-beam implanted Erbium ensembles in Yttrium Orthosilicate crystals by means of confocal photoluminescence spectroscopy. The sample temperature and the post-implantation annealing step strongly reverberate in the properties of the implanted ions. We find that hot implantation leads to a higher activation rate of the ions. At high enough fluences, the relation between the fluence and final concentration of ions becomes non-linear. Two models are developed explaining the observed behavior.

1. Introduction

The development of systems and devices suitable for quantum communication protocols has largely advanced during the last two decades. These systems are optimized for a single application such as data processing, data transmission or data storage. In order to develop a feasible quantum-information infrastructure, it is necessary to combine the best properties of those individual quantum systems within a so-called hybrid system [1,2]. An example of a promising hybrid system is nuclear and electron spins coupled to superconducting resonators and qubits [3–5]. A great leap towards the realization of such an interface had been made in circuit quantum electrodynamics experiments with a variety of spin-ensembles [4,6–12]. Spin-ensembles can be prepared locally on the substrates, thus allowing an arrangement of several bit-units with customized properties on one chip. This enables a simple and available technological process for fabrication of quantum circuits.

We would like to emphasize the ensembles of rare-earth ions (RE) due to their unique properties. The optically active 4f-electrons of the RE elements are semi-shielded from the external fields by the 5d and 6s orbitals, which results in long optical and microwave coherence times. Kramers RE ions possess large magnetic moments, which can be used for the manipulation of their spin states with microwaves. The realization of such spin ensembles by focused ion beam (FIB) implantation technique has many advantages, such as freedom in positioning of different ensembles in one crystal, variability of their concentrations and design of their arrangement in a single mask-less process [13].

One of the crucial requirements for the host substrates is a low local symmetry of the surrounding oxygen ions, which stabilizes the RE ions in the lattice [14,15]. This property is inherent in Y_2SiO_5, $Y_3Al_5O_{12}$, $YAlO_3$ and YVO_4 crystals. In this work, we present in-depth analysis of the FIB-implanted Erbium ensembles in Y_2SiO_5 (YSO) crystals. This crystal is known to have the longest measured optical coherence time of about 4 ms inside the telecom C-band at a wavelength of about 1.5 μm [16,17]. However, formation of defects and dislocations during the implantation process aggravates the optical properties of the ions. Therefore, a deep

---

[*] First corresponding author at: Experimentalphysik, Universität des Saarlandes, D-66123 Saarbrücken, Germany.
[**] Second corresponding author.
E-mail addresses: nadezhda.kukharchyk@physik.uni-saarland.de (N. Kukharchyk), pavel.bushev@physik.uni-saarland.de (P. Bushev).

http://dx.doi.org/10.1016/j.jlumin.2016.05.010
0022-2313/

understanding of ion–matter interactions and activation rates in a particular substrate is indispensable. The first results on the activation rate of the implanted Erbium ensembles have already been reported in Ref. [13].

In this work, we demonstrate a more fundamental analysis of the focused ion beam implanted Erbium ensembles in the Y_2SiO_5 (YSO) crystals in dependence on the preparation process. The implantation of YSO crystals is performed in a wide range of fluences at different temperatures of the substrate. Optical properties of the implanted ions are analyzed in dependence on fluence, ion concentration and ion activation by means of confocal photoluminescence. We compare the results of the photolumisence measurements to the results of microwave spectroscopy of the implanted samples [12].

2. Experimental techniques

Samples: We used crystals supplied by Scientific Materials Inc. The nominally undoped samples were grown by the Czochralski method with a purity of 99.999%, which corresponds to a maximum in situ Erbium presence of 0.0001%. A doped as-grown Er: YSO 0.005% sample was used as a reference.

Focused ion beam implantation: Samples are implanted in a focused ion beam (FIB) machine EIKO-100 with an accelerating voltage of 100 kV under high-vacuum conditions of 10^{-7} mBar. A schematic of the implantation process is demonstrated in Fig. 1(a). In the current work, the FIB operates with a Liquid Metal Alloy Ion Source (LMAIS) $Au_{78.4}Si_{11.6}Er_{10}$ developed by Melnikov et al. [18]. Ions are separated by a built-in Wien mass-filter with a resolution of 2 a.m.u. For the Er^{++} peak, Fig. 1(b), it is possible to make a selection of the isotopic mixture with the lowest content of ^{167}Er (to avoid the spectral broadening from the hyperfine structure). The distribution of the Erbium isotopes relative to the mass spectrum peak is shown in Fig. 1(b).

In this work, the $^{170}Er^{++}$ isotope is implanted with 90% purity. The Wien-filter setting is shown in Fig. 1(b). Implanted fluences vary from 10^{12} cm^{-2} to 10^{16} cm^{-2}. An example of four small implanted patterns is given in Fig. 1(d). Other samples are implanted with larger patterns of 1 mm × 1 mm in size.

For YSO crystals, the sputter rate is low due to the high binding energies of the ions [19,20], i.e. we predominantly implant ions rather than sputter the host crystal. The distributions of ions and induced vacancies are simulated with the SRIM software [21], Fig. 1 (c). As the channelling direction coincides with the D2-axis and is perpendicular to the direction of the ion-beam, Fig. 1(a), the SRIM simulation is applicable for the ion-distribution. From the ion- and defect-profiles, we estimate the final ion-distribution to be 50 nm deep for the ion-density maximum and 32 nm of the ion straggle. For the sample implanted with a fluence of 2×10^{15} cm^{-2}, a Rutherford

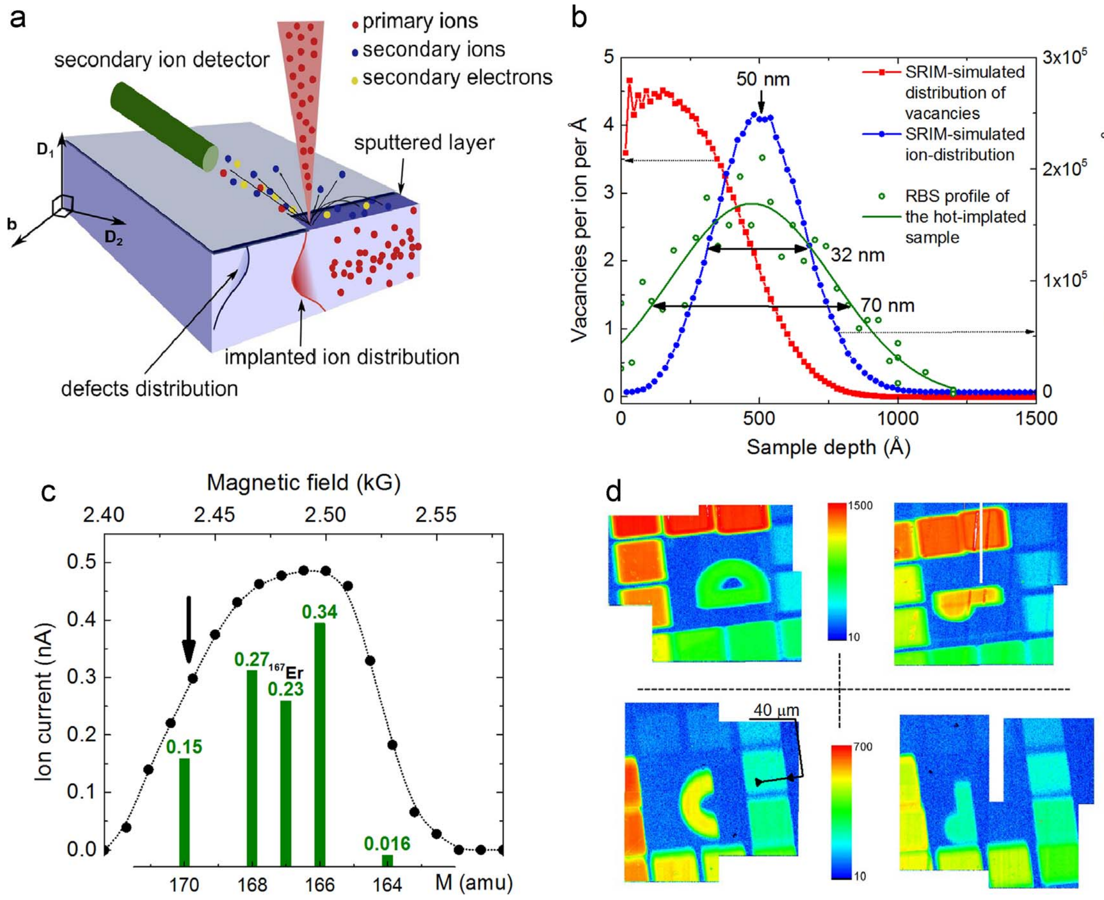

Fig. 1. (a) Schematic of the implantation process. The orientation of the optical symmetry axes is shown accordingly to the sample fabrication and direction of the ion-beam. The ion channelling direction coincides with the D2-axis and is perpendicular to the implantation direction. (b) Mass-spectrum of the Er^{++} peak. The distribution of Erbium isotopes is given by bars according to their natural abundance. The arrow points to the selected position for the implantation. (c) SRIM-simulated data for the ion-distribution (blue) and the vacancy-distribution (red) and RBS measured ion-distribution (green). The RBS result corresponds to the fluence of 2×10^{15} cm^{-2}, below which the concentration is under the detection limit. Depth of the ion-maximum is 50 nm for both SRIM and RBS results. (d) Scanned luminescence pictures of the implanted patterns, intensity in Counts. Letters a, b, c, and d in the middle of patterns correspond to the implantation process as follows: a – implanted at 600 K and annealed; b – implanted at 300 K and annealed; c – implanted at 600 K and not annealed; d – implanted at 300 K and not annealed. (For interpretation of the references to color in this figure caption, the reader is referred to the web version of this paper.)